

On the radio-oxidation, at high doses, of an industrial polyesterurethane and its pure resin



E. Fromentin^{a,*}, C. Aymes-Chodur^b, D. Doizi^a, M. Cornaton^a, F. Miserque^c, F. Cochin^d, M. Ferry^a

^a Den-Service d'Étude du Comportement des Radionucléides (SECR), CEA, Université Paris-Saclay, F-91191, Gif-sur-Yvette, France

^b Université Paris-Sud, SM2B/ICMMO, UMR CNRS 8182, F-91405, Orsay, France

^c Den-Service de Corrosion et de Comportement des Matériaux dans leur Environnement (SCCME), CEA, Université Paris-Saclay, F-91191, Gif-sur-Yvette, France

^d AREVA NC DOR/RDP, 1 Place Jean Millier, F-92084, La Défense Cedex, France

ARTICLE INFO

Keywords:

Polyurethane
Radio-oxidation
High doses
Characterization
Gas
Trapped oxidation products

ABSTRACT

The polymers inside the technological waste packages degrade under radio-oxidation. In the context of the geological nuclear waste storage, the long-term behavior of these polymers must be better understood, especially at high doses. The general objective is to ensure the safety of the geological underground repository.

In this study, we focus on an industrial polyesterurethane, used as glovebox gloves, and its pure resin. These two materials were radio-oxidized at different high doses. The modifications induced by irradiation using low stopping power ionizing rays were assessed through the study of the gas release, the in-chain modifications, and the formation of oxidation products of low molecular mass.

Gas mass spectrometry was used to quantify the gas release with exposure doses up to 4000 kGy for the pure material and 10 000 kGy for the industrial polymer: the evolution with dose is weak and is increasing only in the case of carbon dioxide. The in-chain modifications were identified by infrared spectroscopy or X-ray photoelectron spectroscopy, and correspond probably mainly to the formation of hydroperoxides, hydroxyls and ketones, along with alkenes. By GC-MS or thermodesorption analyses, oxidation products trapped in the polymer matrixes are identified and are esters, carboxylic acids, alcohols, an aromatic molecule and oligomers.

1. Introduction

Organic materials, among which polymers, are present in Intermediate Level Long-Lived Waste (ILW-LL) contaminated with actinides. These polymers are submitted to α , β and γ radiations and their behavior on long time periods, *i.e.* high doses, should be studied for safety purposes. Under ionizing radiations, polymers are modified through the creation of new groups in their backbone, formation of oxidation products of lower molecular mass and gas emission [1,2].

In France, a deep geological repository is being designed, with galleries that will be filled with these waste packages [3]. Because gas released from the radio-oxidized polymers can be explosive and/or inflammable, their production rate must be estimated at least in order to size the forced ventilation used for the alveoli and the galleries. From a safety purpose, the maximal volume of hydrogen allowed to be emitted per year and per package is of 40 NL.¹ The gas release has to be estimated over years, so for doses from non-irradiated to radio-oxidized up to several MGy. The annual dose in a waste package will depend on the design of the waste package: in standard containers of compacted

wastes now under study by AREVA, the absorbed dose is estimated to be about 34 MGy after 300 years [4]. This dose estimation is relatively high compared to other waste packages, such as CBF-C'2 (or F2-3-08), where the absorbed dose is estimated to be about 2 MGy after 300 years [5]. The aim of this article is to access to a better understanding of polyurethane polymers ageing in order to model properly the radiolysis gas release from this family of polymer.

In this study, an industrial aromatic polyesterurethane used as glovebox gloves, is investigated. Among polymers used in the nuclear industry, polyurethane polymers have gained in quantity due to the progressive replacement of poly(vinyl chloride).

Many articles are dealing with polyurethane radio-oxidation or photo-oxidation [6–13]. Polyurethanes are polymers composed of hard segments, which can be aliphatic or aromatic, and of soft segments (generally including the extenders), which can contain ester or ether groups. Walo et al. [14] have shown that the nature of these repetition units is of great importance in the degradation mechanisms encountered under radio-oxidation. For instance, polyurethane with aromatic hard segments is less sensitive to irradiation than polyurethane

* Corresponding author.

E-mail address: elodie.fromentin@cea.fr (E. Fromentin).

¹ NL: Normal Liter (volume at a pressure of 1 bar and a temperature of 20 °C).

with aliphatic hard segments, thanks to the radiation protection effect conferred by the aromatic structure of the hard segments repetition units [15–19]. This phenomenon has already been evidenced in aromatic polyetherurethane by Dannoux et al. [12].

It has also been shown that, whatever their chemical nature, rigid segments are less affected by radio-oxidation than soft segments [20,21]. The more important the length and the concentration of soft segments are, the more sensitive to radio-oxidation the polymer is, and the more modified the mechanical properties of the material are [22].

Only few articles are dealing with aromatic polyesterurethane, *i.e.* polyurethane with aromatic hard segments and ester soft segments. This kind of polymer has been studied under photo-oxidation by Wilhelm et al. [23]. Authors have evidenced the formation of mono- and di-quinone-imides, these molecules being formed from the aromatic hard segments and inducing the yellowing of the polymer. Moreover, they have also observed the homolytic rupture of the C-N bond, leading to the formation of two macroradicals PNH^\bullet and $\text{P}^\bullet\text{O}-\text{C}(=\text{O})$, while a large part of these radicals are undergoing a photo-Fries rearrangement [23,24]. The PNH^\bullet macroradical can also pick up one hydrogen radical and thus form an aromatic amine. In addition, the oxidation of the aromatic hard segments catalyzes the oxidation of the polyester soft segments.

The methylene groups, present in the aromatic hard segments, can release one hydrogen atom, this reaction being followed by a reaction with an oxygen molecule to form peroxy radicals. These last will then form hydroperoxides groups by hydrogen abstraction on another chain [4,23,25]. These hydroperoxides are not stable and will decompose to alkoxy radicals after the O-O bond breakage, which will in turn react by chain scission to form an aldehyde and then a carboxylic acid by reaction with oxygen. Hydroperoxides could also be decomposed to form aromatic acids without intermediate steps.

In some cases, aromatic polyesterurethane have also been studied under radio-oxidation to follow scission to crosslinking ratio. Gel formation dose has been observed at doses as low as 50 kGy in acetone and dichloromethane at a temperature of 33 °C [26]. Moreover, crosslinking concentration increases with dose rate [27,28].

Tian et al. [27] showed by Small-Angle Neutron Scattering (SANS) that the radio-oxidation of an aromatic polyesterurethane decreases the segregation between soft and hard segments. The authors indicate a competition between, on one hand, of the crosslinking formation between segments, bringing together two segments of different nature, and on the other hand, of the increase in the mobility of the segments in the polymer caused by chain scissions. Results obtained on scission to crosslinking ratio are different considering the kind of polyurethanes.

Each kind of polyurethane has a particular behavior under irradiation. The objective of this article is to understand, as much as possible, the radio-oxidation mechanisms that are leading to the ageing of PURm, to be finally able to model the waste package behavior for periods as long as the reversibility period of the French deep geological repository. To obtain information on the fillers and additives effect of this industrial polymer, a pure resin with a chemical composition very close to the industrial polymer but with no fillers nor additives, has also been extensively studied.

2. Experimental

2.1. Materials

2.1.1. Industrial polyesterurethane

The chosen industrial polyesterurethane (named hereafter PURm) is a material used as glovebox gloves, shaped like a film of 0.5 mm thick. The characterization of this polymer has been realized and already presented in a previous article [29].

The resin of PURm is composed of three units that are presented in Fig. 1: 4,4'-methylene diphenyl diisocyanate (MDI), 1,4-butanediol (BDO) and poly(1,4-butylene adipate) (PBA). Hard segments represent

25.5 %wt of the polymer formulation, whereas extenders and soft segments represent 63.4 %wt. Contrary to what is written in the previous article [29], the polymer formula in the industrial material can be written as $(\text{MDI})_{0.20}(\text{PBA})_{0.57}(\text{BDO})_{0.23}$. As we will see in section 2.1.2, the PURm formula previously given in the last article is the one of the pure resin PURE chosen to evaluate the effect of the presence of fillers and additives on the degradation of PURm.

The manufacturer indicates that inorganic additives (probably mainly composed of SiO_2) represent 8.9%wt of the formulation. The remained 1.8 %wt are crosslinking agents and 0.4 %wt corresponds to white and green pigments. The identification of the fillers and additives present in the industrial polyesterurethane was, at least partially, realized by methanol extraction followed by mass spectrometry analyses (GC-MS and ESI-MS). Molecules identified and their role are given in Table 1.

The weight average molecular weight M_w is of 200 000 $\text{g}\cdot\text{mol}^{-1}$ in equivalent polystyrene and the polydispersity index I_p is of 2.8 with a 10% uncertainty value. Finally, the glass transition temperature T_g is equal to -32 ± 5 °C and this polymer is totally amorphous because of the absence of melting peak on the differential scanning calorimetry spectra in the scanned temperature range.

2.1.2. Choice of the corresponding resin and comparison with the industrial material

To evaluate the effect of the presence of fillers and additives on the degradation of the industrial polymer, a model resin, PUR Estane® 5703 (noted hereafter PURE), was identified and furnished by Lubrizol (Belgium).

The three repetition units are the same as the industrial one, and the resin formula can here be written as $(\text{MDI})_{0.17}(\text{PBA})_{0.63}(\text{BDO})_{0.20}$. The weight average molecular weight M_w is 140 000 $\text{g}\cdot\text{mol}^{-1}$ in equivalent polystyrene and the polydispersity index I_p is 2.5 with a 10% uncertainty value. Finally, PURE presents a glass transition temperature T_g equal to -33 ± 1 °C and is also totally amorphous.

Except for the fillers and additives, the resins of PURE and of PURm, although non-identical, are really similar because they present the same extender, soft and hard segments in close ratios. Thus, it can be considered in the following that PURE is a good model polymer of PURm.

2.2. Irradiation

2.2.1. Polyesterurethanes oxidation critical thickness and shaping

To obtain representative irradiations, radio-oxidations have to be performed homogeneously. The radiation-induced oxidation distribution in the depth profile is known to be limited by oxygen availability through diffusion. This oxygen availability is the result of a competition between its permeation through the polymer, and its consumption under irradiation.

The critical thickness, L_c , is the thickness within which the oxidation profile is almost flat (thickness below which the integrated oxidation across the sample will be greater than 90% of the homogeneously oxidized result), and can be estimated following [30]:

$$L_c = \sqrt{8 \cdot \frac{P(O_2) \cdot p}{G_{-O_2} \cdot d}}$$

In this equation, $P(O_2)$ is the oxygen pressure, *i.e.* 0.207 atm. d is the dose rate in $\text{Gy}\cdot\text{s}^{-1}$, G_{-O_2} is the oxygen consumption radiation chemical yield in $\text{mol}\cdot\text{J}^{-1}$, and p is the oxygen permeation coefficient in $\text{mol}\cdot\text{cm}^2\cdot\text{g}^{-1}\cdot\text{atm}^{-1}\cdot\text{s}^{-1}$. p has been experimentally measured on the industrial polymer at the European Institute of Membranes and is equal to $6.32 \cdot 10^{-13} \text{ mol}\cdot\text{cm}^2\cdot\text{g}^{-1}\cdot\text{atm}^{-1}\cdot\text{s}^{-1}$. G_{-O_2} has been determined in the laboratory and is equal to $5.6 \cdot 10^{-7} \text{ mol}\cdot\text{J}^{-1}$, at a dose rate of 1 $\text{kGy}\cdot\text{h}^{-1}$.

In these conditions, the critical thickness calculated is of 0.8 mm: PURm films having a thickness of 0.5 mm, the radio-oxidation is

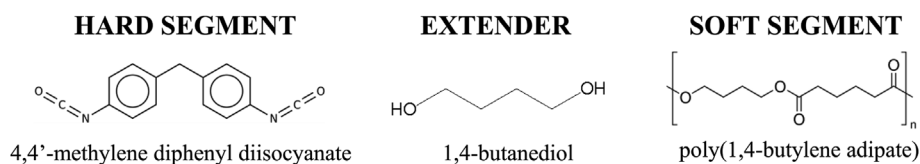
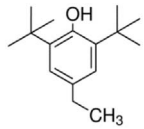
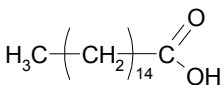
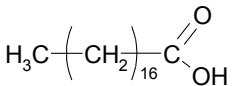
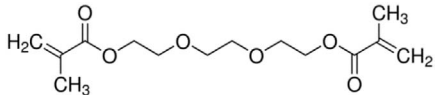
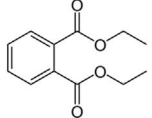
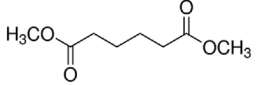
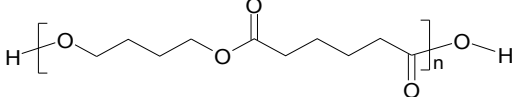
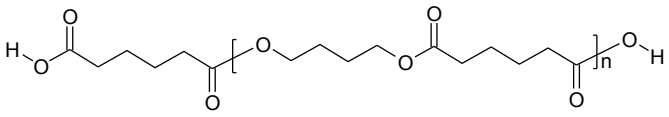
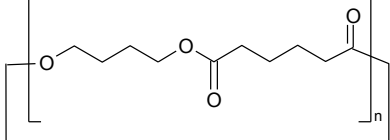
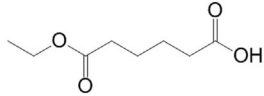
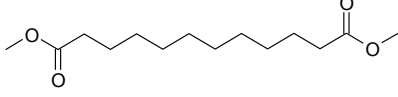


Fig. 1. Chemical formula of the three segments composing the polyesterurethane studied here.

Table 1
Additives and synthesis residues identified in PURm.

Molecule	Proposed structure	Function
2,6-di- <i>tert</i> -butyl-4-ethyphenol		Antioxidant
Palmitic acid		Lubricant & antiadhesive
Stearic acid		Lubricant & antiadhesive
Tri(ethylene glycol) dimethacrylate		Crosslinking agent
Diethyl phthalate		Plasticizer
Dimethyl adipate		Plasticizer and/or synthesis residue
Poly(butylene adipate) n comprised between 1 and 4		Synthesis residue
Poly(butylene adipate) n comprised between 2 and 3		Synthesis residue
Lactonised poly(butylene adipate) n comprised between 1 and 5		Synthesis residue
Monoethyl hexanedioate		Synthesis residue
Dimethyl dodecanedioate		Synthesis residue

homogeneous under the conditions of this study. The industrial polymer is simply cut and irradiated without further shaping. The pure resin polymer, PURE, has been received as granules. Their thickness is too high to ensure a homogeneous radio-oxidation: they were dissolved in tetrahydrofuran (THF) at 60 °C and the obtained solution has been deposited on polytetrafluoroethylene (PTFE) molds. After THF evaporation, PURE films have a thickness of $200 \pm 40 \mu\text{m}$, which is less than the estimated oxidation critical thickness at $1 \text{ kGy}\cdot\text{h}^{-1}$. This result

ensures that radio-oxidation was realized under homogeneous conditions for this polymer too.

2.2.2. Polyesterurethane pre-irradiation

In this study, gamma irradiations were performed by IONISOS or at LABRA in function of the availability of these irradiators. The two industrial irradiators are equipped with a ^{60}Co source. Samples were exposed at room temperature under air in open pillboxes. A glass

Table 2

Irradiator used, polymer radio-oxidized, mean dose rate (inkGy.h⁻¹) and mean dose (in kGy) in this study.

Irradiator	Radio-oxidized polymer	Mean dose rate (kGy.h ⁻¹)	Mean dose (kGy)
LABRA	PURm	0.81	506
IONISOS	PURm	0.74	508
LABRA	PURm	0.79	1004
IONISOS	PURm	0.57	1020
IONISOS	PURm	0.93	4209
IONISOS	PURm	0.69	10 027
IONISOS	PURe	0.78	535
IONISOS	PURe	0.58	1001
IONISOS	PURe	0.93	4209

crystallizer is disposed on the top of each pillbox to prevent from dust of the surrounding irradiation room to deposit on the samples, while allowing air to flow inside the container.

Dosimetry was performed on each sample holder. Irradiation doses and dose rates are given in Table 2. Uncertainties on given doses are less than 6%.

For ease of reading, the round values of the dose will be used in the following sections.

2.2.3. Gas released identification and quantification

Gas released are representative of the first modifications induced by irradiation: it is thus really interesting to follow their evolution to understand the mechanisms involved.

The methodology employed to quantify the gases emitted as a function of the radio-oxidation dose has already been presented in previous articles [31,32]. There are two steps in this method. In a first step, polymers are radio-oxidized, as presented in section 2.2.2. In a second step, there is a dose increment which allows the calculation of the instantaneous production yield. In this second step, PURm and its resin PURe are placed in glass sealed ampoules, under around 700 mbar of pure helium in case of irradiations under inert conditions or of reconstituted air (20.0% O₂, 77.99% N₂, 2.01% Kr) in case of irradiations under oxidative conditions. In this latter case, krypton was used as a tracer and enabled to determine the final pressure. Sample masses were estimated to obtain, at the end of the irradiation, a final H₂ content of about 1%_{vol}.

In the case of the second step, *i.e.* the dose increment, PUR were irradiated in glass sealed ampoules at two different low doses (about 50 and 100 kGy in this study). As we will see in Table 3 in the “Results and discussion” section, some instantaneous gas emission rates are given at zero dose. These points indicate measurements on pristine polymers in glass sealed ampoules, without pre-irradiation. The results are equivalent to the radiation chemical yields extrapolated at zero dose. In the case of this work, the irradiations in glass sealed ampoules were performed at GAMMATEC, equipped with a ⁶⁰Co source. Uncertainties on given doses are less than 6%.

Gas analyses were performed using a quantitative gas mass spectrometer Thermo Fischer Scientific MAT-271 [33]. The instantaneous gas emission rate $\frac{1}{a} \cdot \frac{d[H_2]}{dt}$, in mol.J⁻¹, is obtained using the following equation:

$$\frac{1}{a} \cdot \frac{d[H_2]}{dt} = \frac{P_f \cdot \%_{vol} \cdot V_{free}}{R \cdot T \cdot \Delta D \cdot m}$$

d is the dose rate in Gy.s⁻¹, $[H_2]$ the hydrogen concentration in mol.kg⁻¹ measured after irradiation at a given dose ΔD , P_f the total pressure in the glass ampoule at the end of the irradiation in Pa, $\%_{vol}$ the gas volume fraction determined by gas mass spectrometry, V_{free} the free volume in the glass ampoule in m³, R the gas constant, T the sample's temperature under irradiation in K, ΔD the dose deposited during the second step in Gy, and m the mass of the irradiated sample in kg. The

equation is the same for the other gases, *i.e.* CO₂, CO and CH₄.

For each pre-irradiation dose and each irradiation type, two ampoules were irradiated during the second step. From these experiments, gas instantaneous emission rates are calculated using the equation just above and averaged from the two ampoules. Standard deviation is determined is always less than 10% for hydrogen release.

Between the two irradiation steps, samples are stored under inert atmosphere in the dark to prevent or at least reduce further ageing due to photolysis or photo-oxidation.

Using this two-step procedure presents great advantages [34]. For instance, it prevents gas accumulation (H₂ back reactions) and/or the total consumption of oxygen during irradiation.

2.3. Solid characterization

To evaluate the modifications that were induced in films by the irradiation, different analytical tools were employed. TGA and ultimate analyses were used to follow the global chemical evolutions of the materials, while ATR-FTIR and XPS were employed to follow the new bonds formed in the samples.

2.3.1. Attenuated total reflectance - Fourier Transform InfraRed spectroscopy (ATR - FTIR)

Fourier Transform InfraRed spectra of the polymers were acquired using a Bruker Vertex 70 spectrometer with a Specac Golden Gate single reflection diamond ATR accessory. Detector used is a DTGS (Deuterated TriGlycine Sulfate) and acquisition was recorded between 4000 and 600 cm⁻¹ with a resolution of 2 cm⁻¹.

Although being a non-quantitative method in the conditions of this study, this technique is chosen for its easiness of use, as no sample preparation is needed. Moreover, it gives significant information on the molecular bond nature evolution.

2.3.2. Thermogravimetry (TGA)

Thermograms were recorded with a Netzsch STA 449 F3 Jupiter[®] apparatus, equipped with a SiC furnace and a sample holder in alumina. The heating rate used in this study is 5 °C.min⁻¹, and the gas flow rate is 40 mL.min⁻¹. In all analyses, thermograms were recorded under inert atmosphere (helium) up to 700 °C and under oxidative atmosphere (79.1% N₂ and 20.9% O₂) from 700 °C to 800 °C.

Running under oxidizing conditions allows the graphite carbon, formed during the thermolysis step, to react with O₂ and to form CO₂. Hence, at the end of the thermogravimetric analysis, only inorganic additives remain in the alumina crucible.

2.3.3. X-ray photoelectron spectroscopy (XPS)

XPS analyses of the industrial polyesterurethane samples were carried out with a Thermofisher Escalab 250 XI spectrometer using a monochromatic Al K α X-ray source. Due to important charge effect, the samples were analysed using a dual beam charge compensation flood gun. The instrument was calibrated in energy to the silver Fermi level (0 eV) and to the 3d_{5/2} core level of metallic silver (368.3 eV), the uncertainties on peaks energy being of 0.3 eV. The C-1s signal was used to correct the charge effect: The C-C/C-H component of C-1s spectra was fixed at 285.0 eV. The analysis zone was a 900 μ m diameter spot for the monochromatic source. The pass energy for overview and high resolution spectra was 150 eV and 20 eV, respectively. The data processing was performed using the commercial Avantage software. For the fitting procedure, a Shirley background has been used and Lorentzian-Gaussian (L/G) ratio was fixed at 30%.

2.3.4. Ultimate analysis

Ultimate analysis of the organic elements present in the polymers of this study was realized by the FILAB society. Atomic percentages of carbon, hydrogen and nitrogen were determined using thermal conductivity. Atomic percentages of organic oxygen and sulfur were

quantified by infrared spectroscopy.

2.4. Trapped oxidation products characterization

To extract and identify oxidation products of low molar mass that are trapped in the polymers, different techniques have been developed. Thermal desorption consists in the heating of the samples to desorb the molecules and in analyzing them directly by GC-MS. Another complementary test consisted in the extraction of these molecules using a solvent, methanol in our conditions. Solutes extracted were analyzed using GC-MS, ESI-MS and APCI-MS.

2.4.1. Thermal desorption coupled to gas chromatography - mass spectrometry (TD-GC-MS)

Measurements were performed on a Perkin Elmer thermodesorber (TurboMatrix 350 ATD) connected to the GC-MS presented in section 2.4.2. About 10 mg of polymer were heated at 700 °C during 30 min under helium atmosphere, then desorbed molecules were injected in splitless mode in the injection nozzle heated at 200 °C. Molecules are separated with a CP-PoraBOND Q column 25 m × 0.32 mm × 5 µm and analysed with the mass spectrometer by electron impact over a mass range of 30–300 amu.

The temperature program (initial stabilisation, gradient and final stabilisation) is the same as in the previous section. Helium was used as the carrier gas at a flow rate of 1.7 mL.min⁻¹.

2.4.2. Gas chromatography - mass spectrometry (GC-MS)

Measurements were performed on an Agilent gas chromatography (GC-6890) coupled with a mass spectrometer (MS5973 N). About 1 µL of solution was injected in splitless mode. The inlet temperature was at 250 °C. Molecules are separated on an Agilent CP SiL 5 CB column 25 m × 25 mm × 0.25 µm and analysed with a mass spectrometer equipped with an electron impact source. The MS detector operated in scan mode over a mass-range of 50–300 amu.

The oven was stabilized at 60 °C for 5 min, then a temperature gradient of 7.5 °C.min⁻¹ is applied up to 200 °C and finally maintained at 200 °C for 15 min. Helium was used as the carrier gas at a flow rate of 1.6 mL.min⁻¹.

2.4.3. Electrospray Ionization - mass spectrometry (ESI-MS)

The Q-ToF II Micromass (Waters, Manchester, UK) mass spectrometer is equipped with an Electrospray Ionization (ESI) source and a

accomplished using MassLynx Software (Waters, Manchester, UK).

2.4.4. Atmospheric Pressure Chemical Ionization - mass spectrometry (APCI-MS)

The LCT XE Premier (Waters, Manchester, UK) mass spectrometer is equipped with an Atmospheric Pressure Chemical Ionization (APCI) source and a time-of-flight analyzer. The APCI was operated in the positive ion mode. The capillary voltage was set to 2100 V and 30 V for the sample cone voltage. The source temperature was at 120 °C and the APCI probe temperature at 300 °C. All data analysis was accomplished using MassLynx Software (Waters, Manchester, UK).

3. Results and discussion

The molecular changes induced by ionizing radiations in a polymer can be of several types [35]: crosslinking and chain scissions, emission of volatile compounds (hydrogen H₂, carbon oxides CO and CO₂, hydrocarbon molecules like methane CH₄ ...), creation of new bonds in the macromolecular chain (like unsaturated bonds C=O or C=C, hydroperoxides, peroxides ...) and formation of oxidation products of low molecular mass, trapped in the solid matrix.

The objective of this section is the identification and as far as possible the quantification of these molecules formed in the radio-oxidized PURm and PRe.

3.1. Quantification of instantaneous gas emission rates

Because released gases are the signature of the first modifications induced by the irradiation, analysis of the volatile compounds emission is important. In this section, irradiations are performed in two steps to collect gases. This irradiation in two steps presents advantages given in section 2.2.3 but allows, more than the other advantages, to be sure to perform irradiations under homogeneous oxidative conditions.

Table 3 gives instantaneous gas emission rates obtained from both PUR irradiated at room temperature under gamma-rays and under different atmospheres. Only the four main gases quantified from the polymers are presented here. Other gases were also identified and quantified, but in a lesser extent: less than 15 %_{vol}. They are essentially very low molecular mass alkanes, alkenes and water. As polyesterurethanes contain amine bonds, nitrogen oxides (NO_x) were followed: it can be confirmed here that these gases are absent from the gaseous radio-oxidation products.

Table 3

Instantaneous gas formation rates obtained from PURm and PRe irradiated at room temperature under gamma-rays and under inert or oxidative atmosphere. If radio-oxidation dose is given at zero, then irradiation is directly in closed containers to quantify gases.

Radio-oxidized polymer	Radio-oxidation dose (kGy)	Gas quantification dose (kGy)	Atmosphere in the second step irradiation	Instantaneous gas formation rates (10 ⁻⁷ mol.L ⁻¹)			
				H ₂	CO ₂	CO	CH ₄
PURm	0	49/100	Helium	0.20	0.18	0.19	0.048
	0		Reconstituted air	0.23	0.38	0.20	0.017
	500		Reconstituted air	0.25	0.65	0.24	0.015
	1000		Reconstituted air	0.25	0.72	0.24	0.010
	4000		Reconstituted air	0.18	1.1	0.21	0.014
	10 000		Reconstituted air	0.17	1.4	0.30	0.021
PRe	0	49/100	Helium	0.26	0.15	0.20	0.009
	0		Reconstituted air	0.25	0.51	0.37	0.005
	500		Reconstituted air	0.26	0.81	0.26	0.002
	1000		Reconstituted air	0.26	0.79	0.24	0.002
	4000		Reconstituted air	0.26	1.0	0.25	0.003

time-of-flight analyzer. The ESI was operated in the positive and negative ion modes. The capillary voltage was set to ± 2100 V and the sample cone voltage at ± 50 V. The source temperature was at 80 °C and the temperature of desolvation was 150 °C. All data analysis was

Table 3 allows to study, for non-previously irradiated polymers, the effect of the atmosphere of irradiation on these materials. In both conditions, hydrogen radiation chemical yield extrapolated at zero dose is not influenced by the presence of oxygen in the surrounding

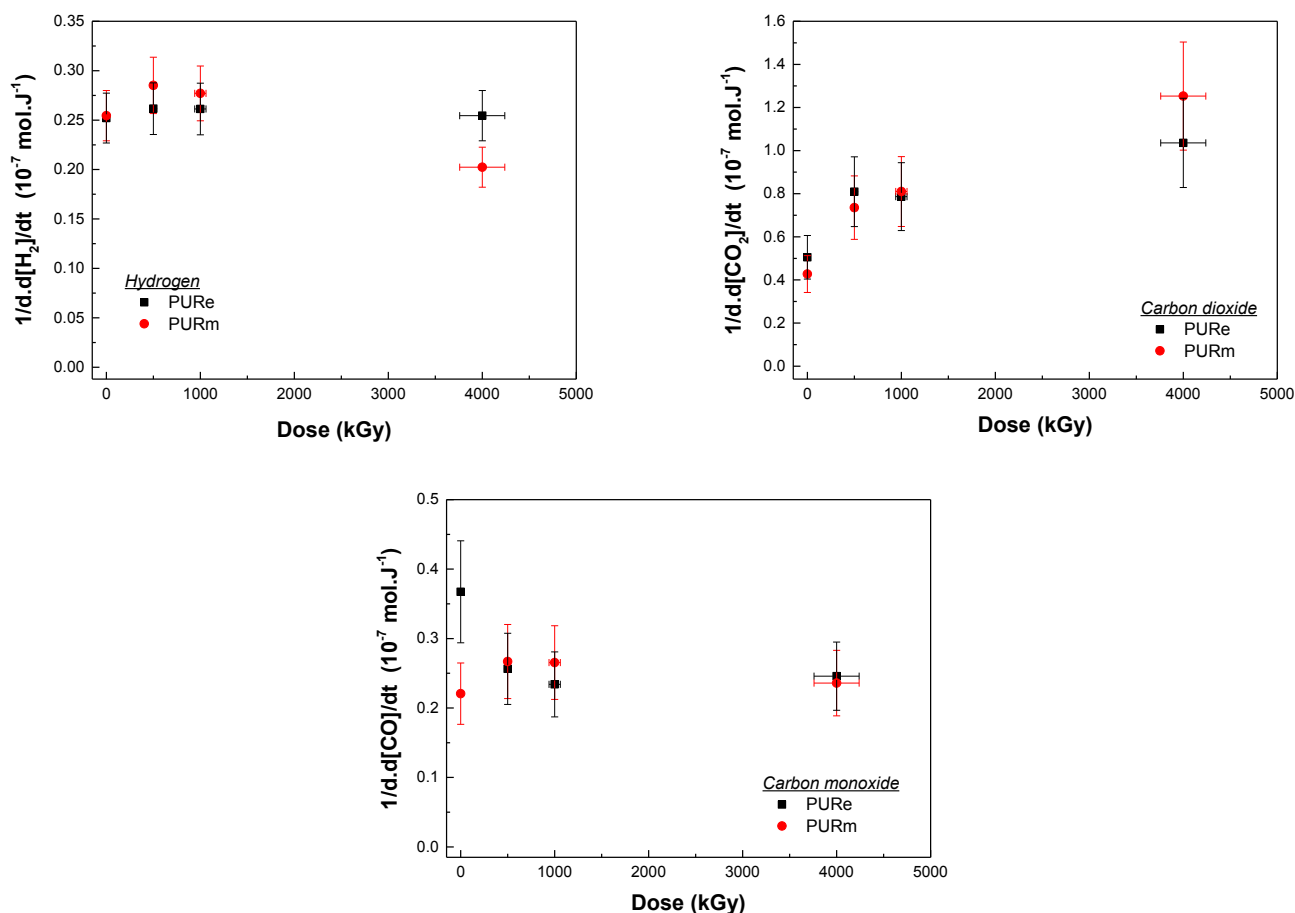


Fig. 2. Different instantaneous gas emission rates evolved from PURe and PURm as a function of dose. On top left, hydrogen emission. On top right, carbon dioxide release. Bottom, carbon monoxide emission. Ordinate error bars correspond to the variation between the two ampoules of the same sample. Abscissa errors correspond to the dose uncertainty (6%).

atmosphere. This observation implies that the reactivity of free radicals leading to the formation of H_2 is extremely high. Moreover, presence of oxygen increases the carbon oxides radiation chemical yields and decreases the methane formation. The methane formation decreases under oxidative conditions, which could be due to methane oxidation. In presence of oxygen, some radicals formed in the polymer during the irradiation will react preferentially with oxygen. This implies that their reactivity is sufficiently low to allow their escape from the spurs² [36] and allow the oxygen to react with them.

Fig. 2 presents the different instantaneous gas emission rates evolved from PURe and PURm at different doses. In case of PURm, the data have been divided by the quantity of resin in the polymer, which explains the slight difference between data of Table 3 and of Fig. 2 for this industrial material. It can be observed on Fig. 2 that the difference between PURm and PURe is not relevant. The only value that is distinct for the two materials is the CO radiation chemical yield extrapolated at zero dose. This slight effect is probably due to the antioxidant, present in PURm as presented in Table 1. Moreover, as they are of sacrificial type, it is not surprising to observe their effect only at low doses. Up to 4000 kGy, there is no dose effect on hydrogen and carbon monoxide release, whatever the material irradiated.

Carbon dioxide release increases strongly with dose. This phenomenon is due to the formation of carboxylic acid groups under radio-oxidation [37] which are further degraded and are released under the form of gaseous CO_2 when dose increases. An electron capture could explain these acids decomposition.

The stability of these two polymers under radio-oxidation is more important than some common polymers used in the nuclear industry, like polyethylene. In this last material, the instantaneous H_2 emission rate is decreased by a factor of about two at a dose as low as 500 kGy [31]. This effect can in part be attributed to the presence of aromatic rings in the hard segments, which confers an important stability to the polymers under ionizing rays [12,18,38–40]. This effect can also in part be due to the quantity of groups initially present in the polymeric chain and which behave as energy and/or radicals scavengers. Above a certain concentration which could be already attained in this kind of polymers, a saturation trend is observed, because of an interpenetration of the protection spheres of each scavenger present [31].

3.2. Materials evolution

To evaluate the effect of the irradiation on both PUR, ultimate analysis of the organic elements present in the materials was realized as a function of dose. Results are given in Table 4 and show an important evolution of the materials when dose increases.

A decrease of the atomic content of carbon, hydrogen and nitrogen is observed while oxygen increases. Taking into account the uncertainties, it can be observed that the behaviors in the case of the pure resin and in the case of the industrial material are more or less equivalent. This observation can be compared with the one obtained on the analysis of gases released where only a small difference, and only on the emission of carbon monoxide, has been observed.

Between 0 and 4000 kGy, there is almost no evolution of the nitrogen content. This observation, combined to the absence of NO_x gaseous products, tends to indicate that the bond breakages do not take

² A 'spur' is a small zone containing excited and ionized species corresponding to ~100 eV of energy loss.

Table 4

Ultimate analysis of the organic elements present, as a function of dose, in PURm and PURe. Whatever the polymer and the dose analyzed, sulfur weight percentage is inferior to the detection limit, i.e. 0.1%. Uncertainties are $\pm 0.4\%$ for carbon, $\pm 0.2\%$ for hydrogen, $\pm 0.03\%$ for nitrogen, and $\pm 0.35\%$ for oxygen determinations.

Radio-oxidized polymer	Mean dose (kGy)	Organic elements analysis (%weight)			
		C	H	O	N
PURm	0	56.8	6.7	24.3	3.2
	500	56.7	6.7	24.3	3.2
	1000	56.5	6.6	24.6	3.2
	4000	55.3	6.4	26.4	3.2
	10 000	53.8	6.2	28.2	3.0
PURe	0	61.9	7.3	28.1	2.5
	500	61.4	7.3	28.8	2.5
	1000	61.3	7.2	28.7	2.5
	4000	60.0	7.1	30.3	2.5

place at the urethane bonds, or in a very low proportion.

To obtain more precise information on the molecular changes, FTIR spectra have been analyzed. Spectra of PURe and PURm are presented as a function of the dose received on Fig. 3. A formation of a large band, between 3700 and 2700 cm^{-1} , characteristic of the ν_{OH} bond vibration, is observed. Moreover, the band relative to $\delta_{\text{C=O}}$ vibration, between about 1800 and 1650 cm^{-1} , is modified under irradiation. The area of these two bands, divided by the area of a band characteristic of the pristine polymer, have been estimated and are given Table 5. The band

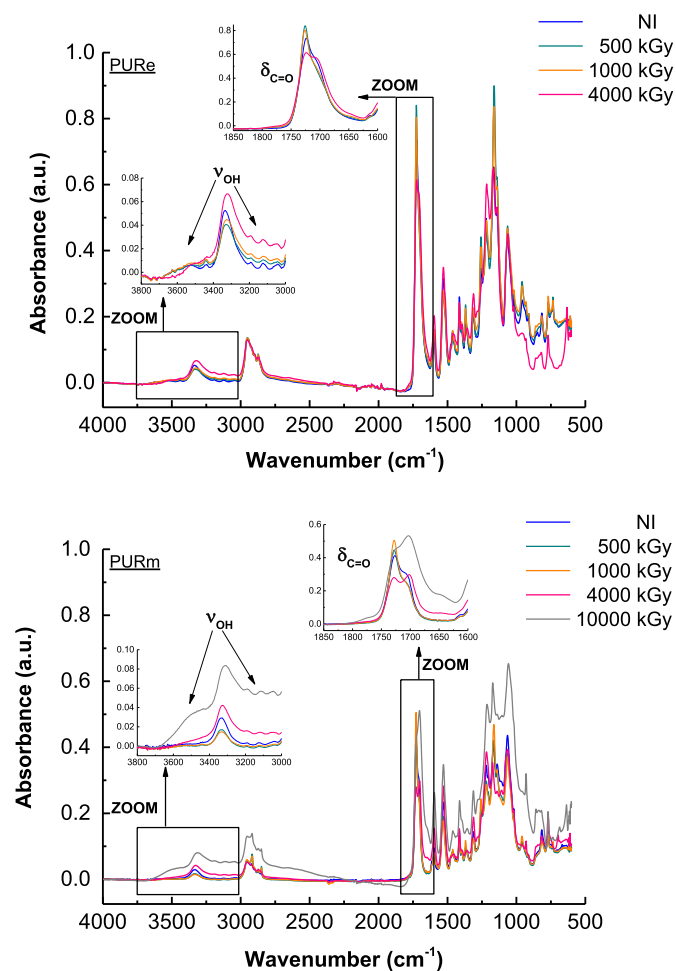


Fig. 3. FTIR-ATR spectra of PURe (above) and PURm (below) as a function of the irradiation dose.

Table 5

Band area ratios. Baseline and area taken at the same wavenumber positions. OH band: $3713\text{--}2382\text{ cm}^{-1}$. C=O and C=C band: $1802\text{--}1626\text{ cm}^{-1}$. Pristine: $1565\text{--}1486\text{ cm}^{-1}$. Band representative of the pristine polymer at 1530 cm^{-1} is representative of C-N stretching and of N-H deformation.

Radio-oxidized polymer	Mean dose (kGy)	Band area			Ratios	
		OH	C=O and C=C	Pristine	OH/pristine	C=O and C=C/pristine
PURm	0	11.4	16.1	5.8	2.0	2.8
	500	11.1	15.2	4.7	2.3	3.2
	1000	11.4	15.8	4.3	2.7	3.7
	4000	19.0	14.5	6.6	2.9	2.2
	10 000	55.7	28.7	8.3	6.7	3.5
PURe	0	29.3	22.2	8.9	3.3	3.7
	500	29.7	32.7	7.4	4.0	4.4
	1000	32.1	32.6	7.6	4.2	4.3
	4000	39.0	33.4	9.7	4.0	3.5

chosen to be representative of the pristine polymer is the one at 1530 cm^{-1} , representative of C-N stretching and of N-H deformation. This band is chosen because it seems, as indicated just above, that the urethane bonds are very stable under these conditions. It is observed that behaviours of the two polymers are similar: new bands ratios are increasing very similarly with dose. The large band representative of -OH increases whatever the dose range, whereas the one representative of C=O and C=C increases up to 1000 kGy and then seems to decrease slightly. This could be an indication of an evolution in the ageing mechanisms, which seems supported by the solubility of both PUR in THF (see Fig. 6, where a modification of the soluble fraction evolution is observed from the same dose).

For PURm radio-oxidized at $10\,000\text{ kGy}$, a shoulder appears upon radio-oxidation at 1790 cm^{-1} and may be attributed to γ -lactones [41]. A band at 1640 cm^{-1} , characteristic of the vinyl C=C bonds is clearly observable. This new band, conjugated to the broadening of the band around 1703 cm^{-1} which could imply the formation of a new band at 1700 cm^{-1} , suggests the formation of conjugated acids like $-\text{CH}=\text{CH}-\text{C}(=\text{O})-\text{OH}$ [42]. This assumption seems supported by the ν_{OH} increase with dose. The ν_{OH} increase is not only ascribable to carboxylic acids: this band refers, more generally, to hydroperoxides and alcohols bonds too.

It can be deduced from the infrared spectra evolutions that, under the radio-oxidation conditions employed in this study, γ -lactones and carboxylic acids seem to be formed, along with alcohols, hydroperoxides, ketones and alkenes. However, very high doses are needed to observe these modifications without any doubt.

To ascertain these bond attributions, C-1s XPS spectra of PURm radio-oxidized at the different doses were registered and are presented on Fig. 4, along with the corresponding deconvolution. The spectrum of the non-irradiated material presents four peaks, whose attributions are the following, with the star presenting the atom which vibrates [43]:

- The peak at 285.0 eV corresponds to C^*-C and C^*-H bonds,
- The peak at 285.7 eV to the C^*-N bonds,

- The one at 286.6 eV to $\text{C}^*-\text{O}-\text{C}-$
 $\begin{array}{c} \text{C}^*-\text{O}-\text{C}- \\ \quad \quad \quad \parallel \\ \quad \quad \quad \text{O} \end{array}$

(but also more generally to $\text{C}^*-\text{O}-\text{C}$ and C^*-OH bonds),

- The last one at 289.2 eV corresponds to $\text{C}-\text{O}-\text{C}^*-\text{O}-$
 $\begin{array}{c} \text{C}-\text{O}-\text{C}^*-\text{O}- \\ \quad \quad \quad \parallel \\ \quad \quad \quad \text{O} \end{array}$

In the kind of polymers of this study, peaks at 286.6 eV and at 289.2 eV should normally have the same intensity for the non-irradiated polymer, which is not the case in this study, as it can be observed on Fig. 4. Some hypotheses could explain this discrepancy. It could first

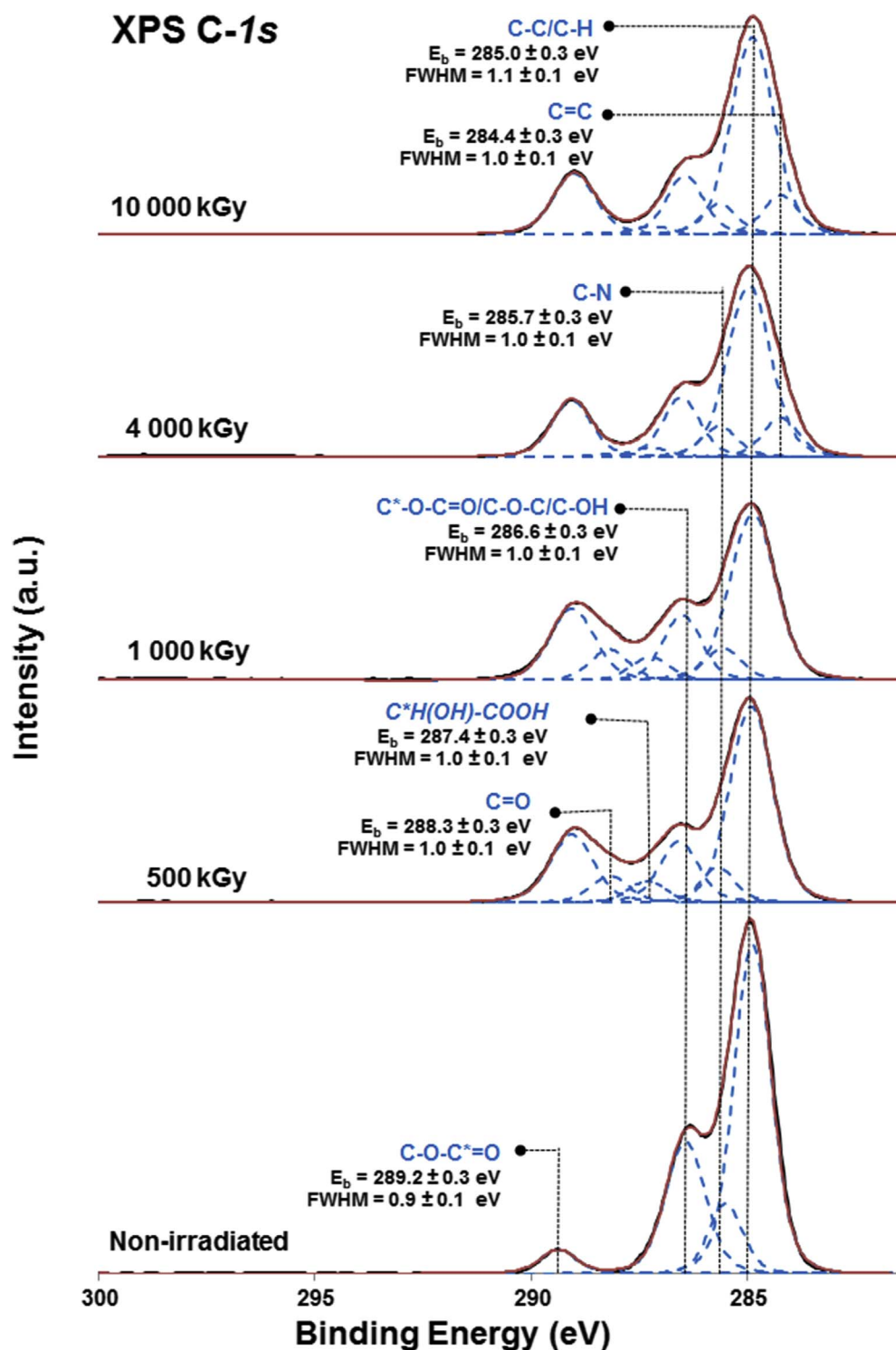


Fig. 4. Deconvolution of C-1s XPS spectra of PURm radio-oxidized at the different doses of this study. From non-irradiated (bottom) to 10 000 kGy (above). Full-Width Half-Maximum (FWHM) is comprised between 0.9 and 1.1 to deconvolute all bands in the same conditions. The attribution in italic, at 287.4 eV, is to be confirmed.

be attributed to the contribution of fillers to the spectrum. This supposition seems invalidated by the nature of the additives identified, more of the ester type than of the ether type in nature (see Table 1). The second supposition is linked to the nature of this analytical tool, which analyses the material, but at the near surface, *i.e.* 10 nm. In these firsts' atomic layers, polymer might present a slight modification at the surface compared to the bulk. The final hypothesis could be a pollution at the surface of the sample. However, even if the first supposition appears unlikely, the last one cannot be discarded. Hence, we will follow only the evolution of the spectra with dose, without quantitative analysis.

With dose, new bands are appearing, whose attributions are known

and are the following:

- Whatever the dose, one new band appears at 288.3 eV, corresponding to C* = O,
- From 4000 kGy, a peak at 284.3 eV rises, corresponding to C* = C.
- Whatever the dose, a new peak at 287.4 eV emerge and its attribution was initially unknown. However, by combining the in-chain new bonds (this section) and the low molecular mass trapped oxidation products (see section 3.3) identified, we are tempted to assume that this bond might be attributable to C*H(OH)-COOH. Further work is in progress to validate this hypothesis.

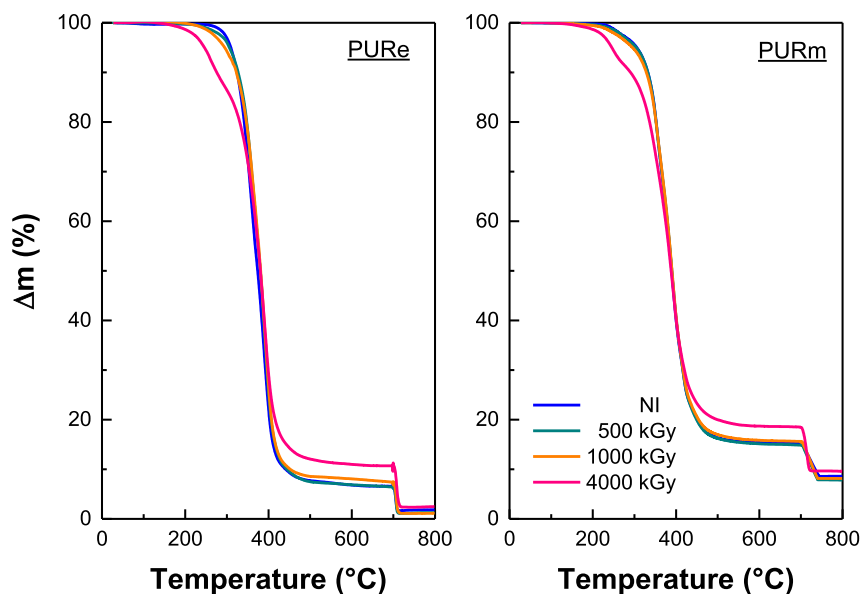


Fig. 5. Thermograms of PURe (on the left) and PURm (on the right) as a function of the irradiation dose.

Table 6

Onset temperature $T_{2\%}$ and maximal degradation rate temperature T_{max} for radio-oxidized PURe and PURm, as a function of dose.

Radio-oxidized polymer	T (°C)	Dose (kGy)			
		Non-irradiated	500	1000	4000
PURe	$T_{2\%}$	291	276	262	214
	T_{max}	/	/	/	258
PURm	$T_{2\%}$	387	386	391	389
	T_{max}	/	/	/	254
PURm	$T_{2\%}$	262	262	249	216
	T_{max}	391	394	389	392

The nature of the new bands identified by XPS give precious information. In fact, $C^* = C$ (284.3 eV), $C^* = O$ (288.3 eV) and maybe $C^*H(OH)-COOH$ correspond to the bands identified using FTIR (in the cases of $C=C$ and $C=O$ bonds formation), and APCI⁺-MS (hydroxyadipic acid, see section 3.3) confirming both attributions.

To follow the evolution of the polymer matrix with dose, thermogravimetric analyses were realized on both polymers. Results are given in Fig. 5 and temperatures of interest are gathered in Table 6. It can be observed that the maximal degradation rate temperature T_{max} is almost unchanged whatever the irradiation dose and the polymer under study. We can however note that at 4000 kGy, a first degradation, at lowest temperature, appears. The temperature of this new degradation step, equivalent for both polymers, indicates a supplementary degradation step which appears when dose increases. This can be also related to the onset temperature at which weight loss reaches 2% (noted $T_{2\%}$): $T_{2\%}$ decreases when dose increases. Finally in the case of PURm, the first degradation step, which represents less than 5%_{wts}, could probably be due to fillers and additives.

Table 6 shows also that $T_{2\%}$ is different for non-irradiated PURm and PURe, whereas it is equivalent in case of polymers irradiated at 4000 kGy. This can be compared to the conclusions concerning the consumption of the additives, presented in section 3.1. It might be deduced that the lower onset degradation temperature in PURm compared to its resin PURe is attributable to additives: at 4000 kGy, most of these molecules are consumed and $T_{2\%}$ is equivalent for both polymers.

The $T_{2\%}$ decrease may also partly be due to the hydroperoxides decomposition. Indeed, it is known that these molecules are formed under radio-oxidation [44] and are unstable even at room temperature

[45]. Finally, desorption and/or evaporation of trapped low molecular mass oxidation products may also be partly involved.

An attempt was done to assess the crosslinking to scission ratio for the two polymers. At room temperature, both non-irradiated PUR are soluble in solvents tested (tetrahydrofuran THF, dimethylformamide DMF, dimethyl sulfoxide DMSO, benzene, cyclohexane, chloroform, dichloromethane, pyridine, 1,4-dioxane and aniline) whereas when irradiated at moderated doses, polymers become insoluble. It can be deduced that in these conditions crosslinking is prevailing. We decided to follow, at different doses, the soluble fraction in THF of PURe and PURm. Fig. 6 presents the results and shows that at low doses, the polymers become partly insoluble: this means that the ratio scissions/crosslinking is decreasing when dose increases. By 500 kGy, this ratio begins to increase when dose increases. At high doses, *i.e.* between 1000 and 4000 kGy for PURe and at about 10 000 kGy for PURm, polymers are again totally soluble in the solvent used here.

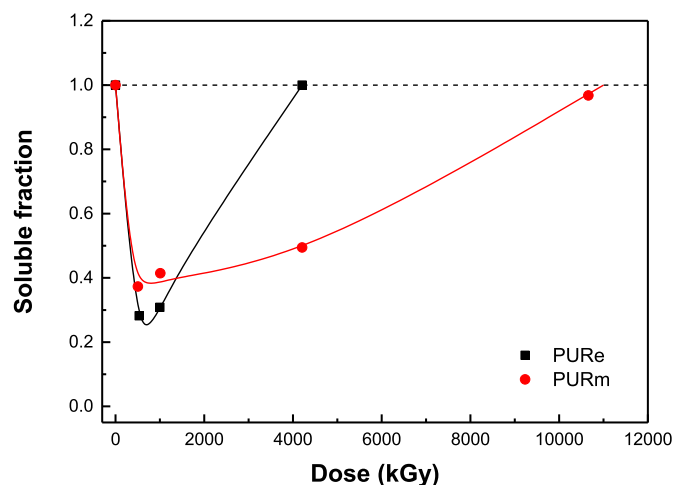


Fig. 6. Soluble fractions in THF at 20 °C of PURe and PURm as a function of the received dose (lines are only to guide the eyes).

The industrial material has a soluble fraction which evolves more slowly than the one of its pure resin, indicating a phenomenon probably due to fillers and additives. It seems that on a mesoscopic scale, the behavior of the polymers is different. Although no analytical technique used in this study allowed to confirm it at a molecular level, it appears that

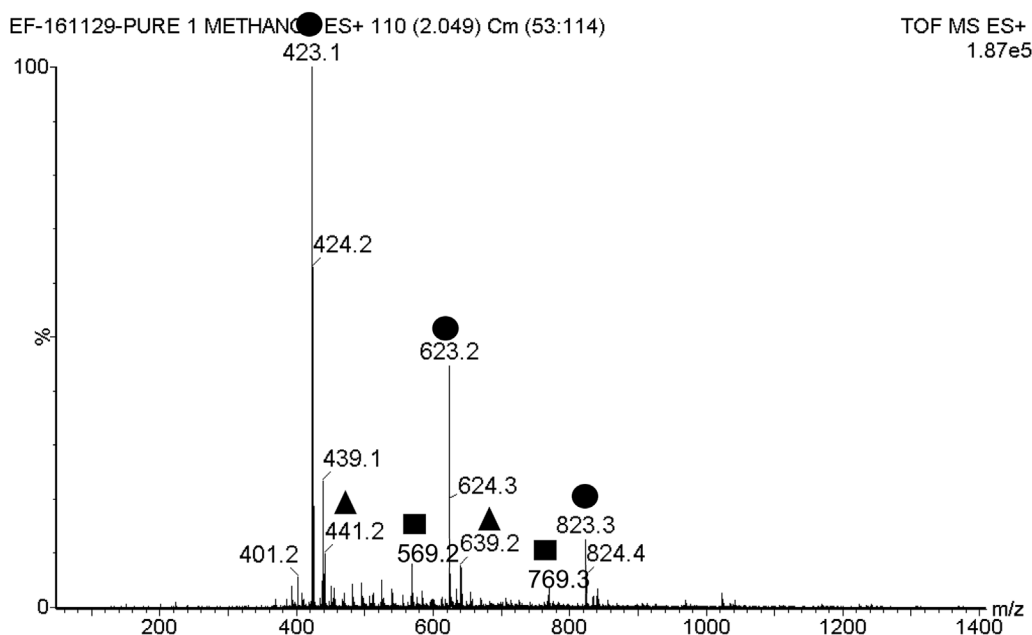
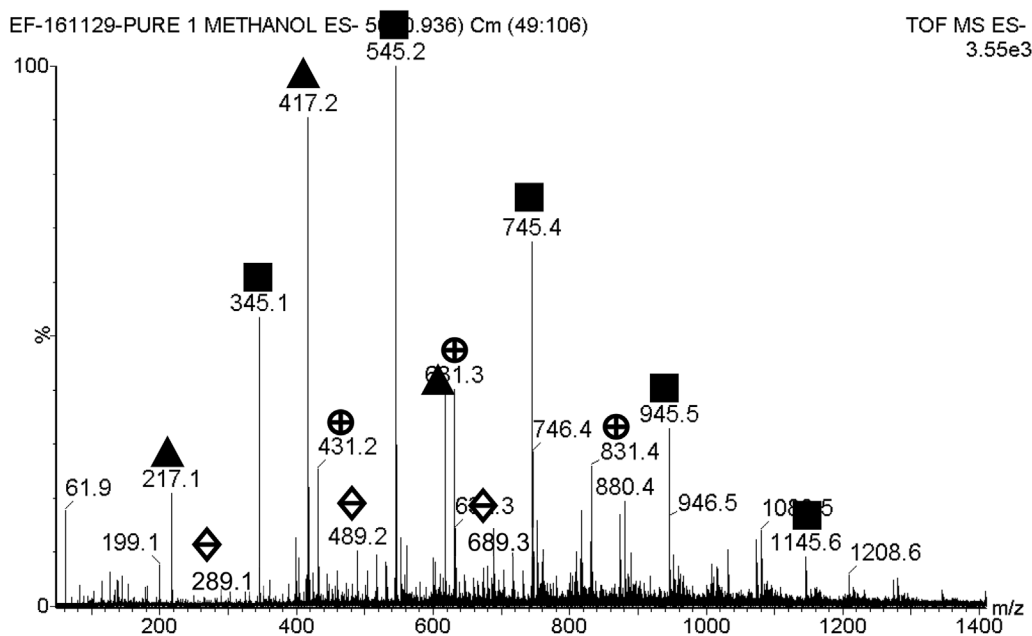


Fig. 7. Mass spectra of the radio-oxidation products issued from PURE irradiated at 1000 kGy. Extraction in methanol. Analyses by ESI+ (above) and ESI- (bottom). Symbols are explained in Table 7.



crosslinking is enhanced by the presence of fillers and additives. Results obtained on PURE at moderated doses are confirmed by the literature, where crosslinking has been evidenced for this polymer [27,28].

3.3. Low molecular mass trapped oxidation products identification

Two different methods were developed to identify these molecules trapped in the polymers: thermal desorption and extraction in methanol, chosen for its polarity. We selected a polar solvent, because of the addition of oxygen in the material evidenced using ultimate analyses: it is probable that the higher the absorbed dose is, the more polar the molecules must be.

As an example, Fig. 7 shows the mass spectra, using ESI and APCI sources in positive and/or negative modes, of the radio-oxidation products released from PURE irradiated at 1000 kGy. Symbols on Fig. 7 represent different families of oligomers. The structures of these oligomers, along with the other molecules identified, are presented on

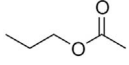
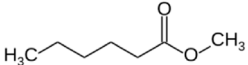
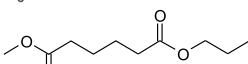
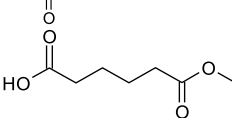
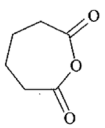
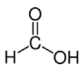
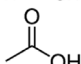
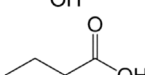
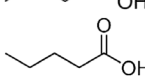
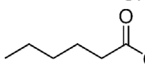
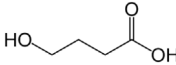
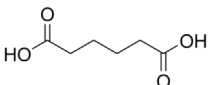
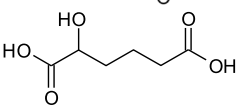
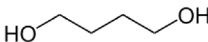
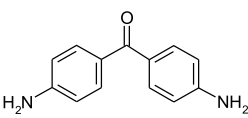
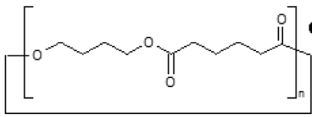
Table 7, which gathers all the results obtained using TD-GC-MS, GC-MS and MS (ESI-, ESI+ and APCI+). Different families of molecules have been identified: esters, carboxylic acids, alcohols, an aromatic molecule, ethers and oligomers issued from soft segments. All these oxidation products are formed by chain scissions. Molecular structures given in Table 7 are only propositions; isomers have also to be considered.

Table 7 shows that for both polymers, radio-oxidation products formed from double scissions in the polymer chain are detected at doses as low as 500 kGy: adipic acid, oligomers and so on. Localization of chain scissions are at random: ester molecules are heterogeneous and come from α , β and γ chain scissions. This result is in concordance with the literature, where scissions have already been observed during the radio-oxidation of polyesters [46–49].

Table 7 shows also the formation of -OH bonds as for instance hydroxyadipic acid. Some unsaturations are also noticeable in one of the oligomers family and butoxybutene. These kinds of molecules with double bonds are rather unusual during radio-oxidation using low

Table 7

Radio-oxidation products identified using TD-GC-MS, GC-MS and MS (ESI-, ESI+ and APCI+), for both polymers radio-oxidized at each dose employed in this study. “X” means that this molecule or family of molecules is suspected to have been formed. “/” Means that the samples concerned have not been analyzed and it is therefore not possible to know whether the molecules concerned are formed at the indicated doses. Symbols from Fig. 7 are explained here. (*): oligomers also detected in non-irradiated polymers but their concentration increases with the absorbed dose.

Molecule Analytical technique used	Proposed structure	PURm				PURE		
		500 kGy	1000 kGy	4000 kGy	10 000 kGy	500 kGy	1000 kGy	4000 kGy
Esters								
Propyle acetate <i>TD-GC-MS</i>					X			
Methyl hexanoate <i>GC-MS</i>				X				
Methyl propyl adipate <i>GC-MS</i>				X				X
Monomethyl adipate <i>GC-MS</i>						X	X	X
2,7-oxepanedione (or lactonized adipic acid) <i>GC-MS</i>				X	X			
Carboxylic acid								
Formic acid <i>TD-GC-MS</i>					X			
Acetic acid <i>TD-GC-MS</i>					X			
Butanoic acid <i>TD-GC-MS</i>					X			
Pentanoic acid <i>TD-GC-MS</i>					X			
Hexanoic acid <i>TD-GC-MS</i>								X
4-hydroxybutanoic acid <i>GC-MS</i>					X			
Adipic acid <i>ESI- et GC-MS</i>		X	X	X	X	X	X	X
Hydroxyadipic acid <i>APCI+</i>		X	X	/	/	/	/	/
Alcohol								
Butane-1,4-diol <i>GC-MS</i>					X			
Aromatic molecule								
Bis(4-aminophenyl)methanone <i>ESI+</i>					X			
Oligomers (issued from soft segments) n comprised between 1 and 5 (*) <i>APCI+, ESI+, GC-MS</i>		X	X	X	X	X	X	X

(continued on next page)

Table 7 (continued)

Molecule Analytical technique used	Proposed structure	PURm				PURE		
		500 kGy	1000 kGy	4000 kGy	10 000 kGy	500 kGy	1000 kGy	4000 kGy
n comprised between 2 and 4 <i>ESI+</i>					X			
n comprised between 2 and 5 <i>APCI + et ESI-</i>		X	X	X	X		X	X
n comprised between 1 and 4 (*) <i>ESI + et ESI-</i>		X	X	X	X	X	X	X
n comprised between 2 and 4 <i>ESI-</i>			X	X	X	X	X	X
n comprised between 1 and 7 <i>ESI+ et ESI-</i>		X	X	X	X	X	X	X
Ethers Butoxybutene <i>ESI+</i>				X	X			

stopping power irradiation but were already described in the literature [4]. The formation of these -C=C- and -OH bonds confirms the infrared bonds attributions. Finally, hydroxyacid and its lactone are both detected by ESI-MS, which is not surprising because this molecule is stable under these two chemical forms [50].

Some carboxylic acids of molecular mass lower than 162 g.mol^{-1} are detected for the industrial polymer radio-oxidized at 10 000 kGy: formic acid, acetic acid, butanoic acid ... these molecules are released from soft segments and extenders [51]. None of the oxidation products or oligomers extracted thermally or using methanol comes from the aromatic hard segments, excepted bis(4-aminophenyl)methanone which only appears in the analysis of the PURm radio-oxidized at 10 000 kGy. Unfortunately, PURE could not be irradiated at the same highest dose. It is concluded that in both PUR studied in this article, scissions may occur slightly preferentially on the -CH₂-O- of the ester bond, which can be attributed to the polarization of the ketone bond. This conclusion is confirmed by the literature [33,52].

It is observed on Table 7 that PURE seems slightly more sensitive than PURm. Identified products are the same for both materials but seem to appear at lower doses in the pure resin. This observation could reinforce the conclusion that some fillers and additives protect the polymer from ageing and degradation at low doses. However, the difference between both polymers is not as important as initially expected.

All the fillers, additives, and residues of synthesis, which have been identified in non-irradiated PURm (see Table 1), are consumed under irradiation. Whatever the irradiation dose, none of these molecules are still present in the irradiated industrial material.

4. Conclusion

Radiolysis stability of an industrial PUR and its resin has been studied. The effect of dose has been evaluated for these polymers by following the gas release, the new bonds formation in the polymeric chain, and identification of low molecular mass oxidation products trapped in the samples.

Instantaneous gas emission rates have been quantified at different doses and have shown that there is no significant effect, on the gas studied release, of fillers and additives present in the industrial polymer. The dose effect can be observed only on the CO₂ release: at

low doses, carboxylic acid groups formation increases with dose. At higher doses, these carboxylic acid groups are then destroyed by energy and/or radicals transfers, and lead finally to CO₂ release.

The physical appearance of the materials changes according to the dose received has also been followed. Formation of carboxylic acids, hydroxyls and alkenes groups has been evidenced. Alkenes formation is surprising because in homogeneous conditions of low stopping power ionizing rays radio-oxidation, only oxidized news groups are usually observed.

The radio-oxidation molecular products were determined. Esters, carboxylic acids, alcohols, an aromatic molecule and oligomers from the soft segments have been identified. Through the identification of these radio-oxidation products, chain scissions are clearly highlighted.

By following the soluble fraction of PURE and PURm as a function of dose, we showed that at low doses, the ratio scissions/crosslinking decreases when dose increases. By 500 kGy, this ratio begins to increase when dose increases. The dose at which the polymer becomes totally soluble again is lower for PURE than for PURm: total solubility is attained between 1000 and 4000 kGy for PURE and at about 10 000 kGy for PURm. Hence, the presence of fillers and additives enhances crosslinking: it seems that on a mesoscopic scale, the behavior of PURm and PURE is different.

In the ILW-LL nuclear waste safety context, both polymers have been radio-oxidized under controlled conditions at doses representatives of those that will be encountered in the French geological repository, during the reversibility period. Gas instantaneous emission rates have been estimated over the dose range and the ageing mechanism has been better understood. By estimating the quantity of the different polymers in the waste packages, the explosive and/or inflammable gas emission quantity can be estimated and the forced ventilation used for the alveoli and the galleries can be scaled. Hence, this work will improve the safety of the foreseen geological repository.

Acknowledgements

EDF is thanked for its financial support. Sophie Rouif from IONISOS, Philippe Le Tutour from LABRA and Véronique Labeled and Maryline Charlot from GAMMATEC are acknowledged for their helpful collaboration during irradiations. Emmanuel Buiret from FILAB is thanked

for his support during the ultimate analyses. Finally, Annick Geysen and Julie Goldberg from Lubrizol are acknowledged for having kindly provided us the pure resin, PUR Estane® 5703. Finally, Solène Legand, Diane Lebeau, Jean-Luc Roujou, Delphine Durand, Vincent Dauvois and Stéphane Esnouf are thanked for their assistance during experiments.

References

- [1] M. Dole, *The Radiation Chemistry of Macromolecules - Volume 1*, Academic Press, 1972.
- [2] A. Chapiro, *Radiation Chemistry of Polymeric Systems*, Interscience Publishers, 1962.
- [3] <http://www.cigeo.com/en/>.
- [4] A. Dannoux, *Extrapolation dans le temps des cinétiques de production des produits de dégradation radiolytique : application à un polyuréthane*, Université Paris XI, Paris, 2007.
- [5] Andra, *Catalogue descriptif des familles. Inventaire national des matières et déchets radioactifs*, (2015).
- [6] C. Wilhelm, J.-L. Gardette, *Polymer* 38 (1997) 4019–4031.
- [7] G.R. Saad, T.M. Khalil, M.W. Sabaa, *J. Polym. Res.* 17 (2010) 33–42.
- [8] K. Gorna, S. Gogolewski, *Polym. Degrad. Stab.* 79 (2003) 465–474.
- [9] D.W. Cooke, R.E. Muenchausen, B.L. Bennett, E.B. Orlor, D.A. Wroblewski, M.E. Smith, M.S. Jahan, D.E. Thomas, *Nuclear Instruments and Methods in Physics Research Section B: Beam Interactions with Materials and Atoms* vol. 151, (1999), pp. 186–189.
- [10] D.W. Cooke, R.E. Muenchausen, B.L. Bennett, E.B. Orlor, D.A. Wroblewski, M.E. Smith, M.S. Jahan, D.E. Thomas, *Radiat. Phys. Chem.* 55 (1999) 1–13.
- [11] A. Dannoux, S. Esnouf, J. Begue, B. Amekraz, C. Moulin, *Nuclear Instruments and Methods in Physics Research Section B: Beam Interactions with Materials and Atoms* vol. 236, (2005), pp. 488–494.
- [12] A. Dannoux, S. Esnouf, B. Amekraz, V. Dauvois, C. Moulin, *J. Polym. Sci. Part B Polym. Phys.* 46 (2008) 861–878.
- [13] C. Guignot, N. Betz, B. Legendre, A.L. Moel, N. Yagoubi, *Nuclear Instruments and Methods in Physics Research Section B: Beam Interactions with Materials and Atoms* vol. 185, (2001), p. 100.
- [14] M. Walo, G. Przybytniak, J. Sadło, *J. Mol. Struct.* 1036 (2013) 488–493.
- [15] J.A. Stone, P.J. Dyne, *Radiat. Res.* 17 (1962) 353.
- [16] C.S. Schoepfle, C.H. Fellows, *Ind. Eng. Chem.* 23 (1931) 1396.
- [17] J.P. Manion, M. Burton, *J. Phys. Chem.* 56 (1952) 560–569.
- [18] M. Ferry, E. Bessy, H. Harris, P.J. Lutz, J.M. Ramillon, Y. Ngonon-Ravache, E. Balanzat, *J. Phys. Chem. B* 117 (2013) 14497–14508.
- [19] R. Basheer, M. Dole, *J. Polym. Sci. Polym. Phys. Ed.* 22 (1984) 1313–1329.
- [20] G. Przybytniak, E. Kornacka, J. Ryszkowska, M. Bil, A. Rafalski, P. Woźniak, *Nukleonika* 51 (2006) S121–S128.
- [21] R.S. Maxwell, D. Chambers, B. Balazs, R. Cohenour, W. Sung, *Polym. Degrad. Stab.* 82 (2003) 193–196.
- [22] M. Walo, G. Przybytniak, K. Łyczko, M. Piątek-Hnat, *Radiat. Phys. Chem.* 94 (2014) 18–21.
- [23] C. Wilhelm, A. Rivaton, J.-L. Gardette, *Polymer* 39 (1998) 1223–1232.
- [24] G.M. Coppinger, E.R. Bell, *J. Phys. Chem.* 70 (1966) 3479–3489.
- [25] J.F. Rabek, *Photodegradation of Polymers: Physical Characteristics and Applications*, Springer Science & Business Media, Berlin, 1996.
- [26] Y.M. Milekhin, D.N. Sadovnichii, S.V. Mukhachev, A.A. Koptelov, N.I. Shishov, E.A. Butenko, L.A. Davydova, *High. Energy Chem.* 42 (2008) 18–22.
- [27] Q. Tian, E. Takács, I. Krakovský, Z. Horváth, L. Rosta, L. Almásy, *Polymers* 7 (2015) 1755–1766.
- [28] H. Shintani, H. Kikuchi, A. Nakamura, *J. Appl. Polym. Sci.* 41 (1990) 661–675.
- [29] E. Fromentin, M. Pielawski, D. Lebeau, S. Esnouf, F. Cochin, S. Legand, M. Ferry, *Polym. Degrad. Stab.* 128 (2016) 172–181.
- [30] K. Gillen, R. Clough, *Accelerated aging methods for predicting long-term mechanical performance of polymers, Irradiation Effects on Polymers*, Elsevier Applied Science, London, 1991, pp. 157–223.
- [31] M. Ferry, E. Pellizzi, I. Boughattas, E. Fromentin, V. Dauvois, G. de Combarieu, P. Coignet, F. Cochin, Y. Ngonon-Ravache, E. Balanzat, S. Esnouf, *Radiat. Phys. Chem.* 118 (2016) 124–127.
- [32] D. Lebeau, S. Esnouf, J. Gracia, F. Audubert, M. Ferry, *J. Nucl. Mater.* 490 (2017) 288–298.
- [33] M. Ferry, A. Dannoux-Papin, N. Dély, S. Legand, D. Durand, J.L. Roujou, C. Lamouroux, V. Dauvois, P. Coignet, F. Cochin, S. Esnouf, *Nucl. Instrum. Methods Phys. Res. Sect. B* 334 (2014) 69–76.
- [34] D. Lebeau, L. Beuvier, M. Cornaton, F. Miserque, M. Tabarant, S. Esnouf, M. Ferry, *J. Nucl. Mater.* 460 (2015) 130–138.
- [35] J.H. O'Donnell, *The Effects of Radiation on High-technology Polymers*, American Chemical Society, Washington DC, 1989.
- [36] M. Ferry, Y. Ngonon-Ravache, C. Aymes-Chodur, M.C. Clochard, X. Coqueret, L. Cortella, E. Pellizzi, S. Rouif, S. Esnouf, *Ionizing radiation effects in polymers, in: S. H (Ed.), Reference Module in Materials Science and Materials Engineering*, Elsevier, Oxford, 2016, pp. 1–28.
- [37] J. Lacoste, D.J. Carlsson, *J. Polym. Sci. Part A Polym. Chem.* 30 (1992) 493.
- [38] M. Ferry, E. Bessy, H. Harris, P.J. Lutz, J.M. Ramillon, Y. Ngonon-Ravache, E. Balanzat, *J. Phys. Chem. B* 116 (2012) 1772–1776.
- [39] Z. Chang, J.A. LaVerne, *J. Polym. Sci. Part A Polym. Chem.* 38 (2000) 1656–1661.
- [40] Z. Chang, J.A. LaVerne, *J. Phys. Chem. B* 104 (2000) 10557.
- [41] D.J. Carlsson, R. Brousseau, C. Zhang, D.M. Wiles, *Identification of products from polyolefin oxidation by derivatization reactions*, *Chemical Reactions on Polymers*, American Chemical Society, 1988, pp. 376–389.
- [42] N.B. Colthup, L.H. Daly, S.E. Wiberley, *Introduction to Infrared and Raman Spectroscopy*, 3rd Edition, Academic Press Inc., 1990.
- [43] G. Beamson, D. Briggs, *High Resolution XPS of Organic Polymers: the Scienta ESCA300 Database*, John Wiley & Sons, Chichester, 1992.
- [44] A. Rivaton, S. Cambon, J.L. Gardette, *Nuclear Instruments and Methods in Physics Research Section B: Beam Interactions with Materials and Atoms* vol. 227, (2005), pp. 357–368.
- [45] P.L. Hanst, J.G. Calvert, *J. Phys. Chem.* 63 (1959) 104.
- [46] J. Bei, W. He, X. Hu, S. Wang, *Polym. Degrad. Stab.* 67 (2000) 375–380.
- [47] A. Buttafava, G. Consolati, M. Mariani, F. Quasso, U. Ravasio, *Polym. Degrad. Stab.* 89 (2005) 133–139.
- [48] J. Mosnáček, K. Borská, M. Danko, I. Janigová, *Mater. Chem. Phys.* 140 (2013) 191–199.
- [49] U. Ravasio, A. Buttafava, M. Mariani, D. Dondi, A. Fautitano, *Polym. Degrad. Stab.* 93 (2008) 1031–1036.
- [50] L.A. Giolino, M.Z. Mesmer, R.D. Satzger, A.C. Machal, H.A. McCauley, A.S. Mohrhaus, *J. Forensic Sci.* 46 (2001) 1315–1323.
- [51] C. Aymes-Chodur, A. Dannoux, V. Dauvois, S. Esnouf, *Polym. Degrad. Stab.* 96 (2011) 1225–1235.
- [52] A. Babanalbandi, D.J.T. Hill, J.H. O'Donnell, P.J. Pomery, *Polym. Degrad. Stab.* 52 (1996) 59–66.